THE UNIVERSITY OF
WARWICK

Original citation:
Aaronson, Barak D. B., Byers, Joshua C., Colburn, Alex W., McKelvey, Kim M. (Kim Martin) and Unwin, Patrick R.. (2015) Scanning electrochemical cell microscopy platform for ultrasensitive photoelectrochemical imaging. Analytical Chemistry, Volume 87 (Number 8). pp. 4129-4133.
Permanent WRAP url:
http://wrap.warwick.ac.uk/67808

warwick**publications**wrap
highlight your research

http://wrap.warwick.ac.uk/

A Scanning Electrochemical Cell Microscopy Platform for Ultra-sensitive Photo-electrochemical Imaging

Barak D. B. Aaronson, Joshua C. Byers, Alex W. Colburn, Kim McKelvey, Patrick R. Unwin[*]

Department of Chemistry, University of Warwick, Gibbet Hill Rd, CV4 7AL, Coventry, UK

Abstract

Developing nanoscale structure-activity correlations is of major importance for the fundamental understanding and rational development of (photo)electrocatalysts. However, the low conversion efficiency of characteristic materials generates tiny photoelectrochemical currents at the submicron to nanoscale, in the fA range, which are challenging to detect and measure accurately. Here we report the coupling of scanning electrochemical cell microscopy (SECCM) with photo-illumination, to create a sub-micron spatial resolution cell that opens up high resolution structure-(photo)activity measurements. We demonstrate the capabilities of the technique as a tool for: (i) high spatial resolution (photo)activity mapping using an ionic liquid electrolyte at a thin film of TiO_2 aggregates, commonly used as a photo-anode in dye sensitized solar cells (DSSCs); and (ii) in-situ (photo)activity measurements of an electropolymerized conjugated polymer on a transparent Au substrate in a controlled atmospheric environment. Quantitative data, including localized (photo)electrochemical transients and external quantum efficiency (EQE) are extracted, and prospects for further technique development and enhancement are outlined.

Introduction

Photo-electrodes for energy conversion devices typically consist of nanostructured electrodes based on nanoparticles and molecular materials. Not only does this provide substrates with high specific surface area and enhanced light absorbance characteristics, but it also opens up the possibility of fine tuning (photo)electrocatalytic properties including crystallographic orientation, size, film thickness and absorption spectrum.[1] On the other hand, correlating the structure of these materials with their local (photo)activity requires localized (photo)electrochemical measurements capable of sub-micron (nanoscale) spatial resolution where feature sizes of tens to hundreds of nanometers are typical. Furthermore, the small feature sizes as well as the low conversion efficiencies of many (photo)electrochemical systems requires high sensitivity current measurements. As a result, there have been few reports of scanning probe (photo)electrochemical measurements. In fact, these have mainly focused on scanning electrochemical microscopy (SECM) based techniques,[2-11] often as a tool for catalyst screening[4,7] on a fairly large length scale and for thick deposits of photoelectrocatalytic materials.[4,7,12,13]

Here, we use a scanning droplet cell platform that confines the electrochemical measurement to a small contact area[14,15] ensuring high spatial resolution and excellent signal-to-noise,[16] as responses from features outside the probe area are excluded. Although scanning droplet cells have found some recent application for localized photovoltaic measurements on organic materials,[17] the droplet cell in these studies (3.5 mm in diameter)[17] operates with an aerial footprint five orders of magnitude larger than herein. As a member of the scanning droplet technique family,[18] scanning electrochemical cell microscopy (SECCM)[14,18-23] has emerged in recent years as a powerful technique to visualize electrochemistry at the nanoscale as well as to functionalize surfaces.[24,25] Key capabilities of SECCM are mainly due to: (i) a nanoscopic droplet size at the tip of the scanning probe (down to < 200 nm in

2

diameter in published studies[15] and < 100 nm in work in progress in our group) and (ii) an independent feedback mechanism that provides constant tip-substrate separation, unambiguously allowing surface reactivity to be separated from topography.

In this contribution we describe an experimental setup in which photocurrent measurements are incorporated into SECCM, enabling mapping and interrogation of photoelectrochemistry at nanostructured films with high spatial resolution and signal-to-noise ratio. Using a hopping mode technique,[26] localized measurements were performed at multiple locations across heterogeneous substrate surfaces, providing individual photocurrent transient measurements at the micro to nanoscale. As light intensity modulation techniques such as intensity modulated photocurrent spectroscopy (IMPS) are useful in extracting information on the charge transport and recombination processes in photoelectrochemical systems,[27] we also show herein, as a proof of concept, the simultaneous use of a second lock-in amplifier to modulate the light intensity and measure the ac photocurrent at the same frequency.

In order to demonstrate the capabilities of SECCM coupled with illumination, we have selected two energy-related photosystems and developed two different configurations. In the first approach, related to dye sensitized solar cells (DSSCs), (photo)electrochemical imaging of dye sensitized TiO_2 aggregates on a highly orientated pyrolitic graphite (HOPG) substrate was carried out to show the high spatial resolution and high sensitivity of current measurements that is possible using SECCM. In a second approach, electropolymerization of a conjugated polymer poly(3-hexylthiophene) (P3HT) was carried out followed by in-situ (photo)electrochemical characterization, demonstrating the potential for materials fabrication[24,25,28] and in-situ characterization under a controlled environment.

3

Experimental

Photo-SECCM setup

A detailed description of the setup can be found in the Supporting Information (SI), section S1, especially Figure S1. Briefly, a dual channel glass (theta) capillary (Harvard Apparatus, UK) was pulled to a fine tip (450 nm diameter) and filled with the solution of interest (see SI, section S2 for solutions and sample preparation) to form a small meniscus at the end of the tip. Ag wire (0.255 mm 3N, MaTeck), was inserted in each 'barrel' to act as a quasi-reference counter electrode (QRCE), and a bias potential (V_2) was applied between the two QRCEs to induce a conductance current (i_{dc}) through the meniscus which was continuously monitored, providing the basis for the tip-substrate separation feedback mechanism (Figure 1).[18-20] The potential of the substrate was controlled via V_1 (Figure 1), where the potential of the surface (V_{Surf}) is expressed as: $V_{Surf} = -V_1 - V_2/2$.[20] The current through the substrate (i_{Surf}) was continuously recorded with a home-built four decade autoranging current follower, optimized for ultra-low current low noise measurement. A specialized electrometer and an eighth-order brick wall filter allowed the measurement of currents in the range of only tens of fA (SI, section S1). Positional feedback (height of the probe with respect to the surface) was achieved by modulating the probe position with a small amplitude in the direction perpendicular to the surface and a lock-in amplifier to detect the conductance current (i_{ac}) across the droplet at the end of the tip of the scanning probe (essentially independent of surface reactivity).[19,20] For the study of P3HT, the tip and sample were placed in a N_2 purged environmental cell to assist in drying of the meniscus at the end of the tip.[22]

The light source was a cool-white 5,000 – 10,000 K CCT light emitting diode (LED) (Cree XLamp XR-E Series, Cree, USA). The LED intensity could either be set to a fixed dc

value or modulated via an additional external lock-in amplifier giving rise to a measurable ac photocurrent for photoactive surfaces. Unless otherwise stated, the light intensity was modulated. In the case a fixed light intensity illumination was used, the LED intensity was set to the maximum intensity (33 mW cm^{-2}, measured using a laser power meter (Newport, model 407A, USA)).

Results and Discussion

Photo-SECCM hopping scans on dye sensitized TiO$_2$ films

A 9 × 4 µm SECCM scan was performed on a drop-casted sensitized TiO$_2$ film on HOPG with a tip containing I$^-$ (13 mM tetrabutylammonium iodide) in an ionic liquid (1-butyl-3-methylimidazolium tetrafluoroborate [BMIm][BF$_4$]). During scanning, the substrate potential was held at a fixed value of + 0.4 V vs Ag QRCE as determined by linear sweep voltammetry (LSV) under illumination (see SI, section S3). To facilitate localized transient measurements, a hopping mode scan was adopted as illustrated in Figure 2a. Hopping mode scans consisted of a series of approach/retract measurements arranged in a rectangular array at predefined locations in the xy plane of the sample. Each approach/retract measurement is referred to as a 'hop'. The hopping scans were performed with a separation of 1 µm between each point in the *xy* plane, using a probe with a tip diameter (450 nm) that was smaller than the hopping distance to avoid overlap of hop measurements. A bias of + 0.16 V was applied between the QRCEs[18,20,22] resulting in a stable i_{dc} of circa 0.2 nA across the meniscus. Once the surface was detected using i_{ac} as feedback (step 1 in Figure 2a), the tip movement in the *z* direction was halted and a hold time of 4 seconds was maintained (step 2 in Figure 2a). The initial hold time on the surface provided the substrate background measurement under dark conditions. After the initial dark hold time, the LED was turned on for photocurrent

measurements for 4 seconds, which was long enough to reach quasi steady-state (step 4 in Figure 2a). An ac photocurrent was simultaneously generated by modulating the light intensity and measuring the response at the same frequency using a lock-in amplifier. Finally, the tip was retracted from the surface and moved to the next measurement position in the xy plane (step 5 in Figure 2a).

Typical transients (surface current vs time) of hop measurements on a bare HOPG substrate and on photoactive (HOPG with sensitized TiO_2 film) areas are shown in Figure 2b and 3c, respectively. The detection of the surface by the meniscus ($t = 0$) is seen, in both cases, as a sharp spike in i_{Surf}. In both cases (bare HOPG and sensitized TiO_2 areas), the initial 4 seconds hold time under dark conditions, yields a low background current (around 50 fA (peak to peak)), highlighting that extremely low current signals can be measured. No change in surface current is observed for the HOPG region when the light is switched on (Figure 3b), whereas the sensitized TiO_2 (Figure 3c) shows an increase in the surface current upon illumination, reaching a quasi-steady-state of ~ 300 fA, with a rise time of ~ 1.5 second. The rise time of the electrometer was 1 ms (with a sensitivity of 1 pA/V as here), therefore the rise time of the (photo)transient is due to the slow charge transport through the mesoporous TiO_2 thin film, which is much longer than the time constant of the filter (1 ms) and in agreement with bulk measurements.[29,30] The periodic modulation of the dc surface current seen in Figure 2c during illumination corresponds to the 9 Hz ac modulation in light intensity. The ability to clearly follow the periodic modulation in the dc photocurrent, without a lock-in amplifier, highlights the combined high sensitivity and reasonable bandwidth of the electrometer used herein. Finally, at $t = 8$ s the tip is retracted from the surface at a rate of 1 $\mu m\ s^{-1}$.

A field emission scanning electron microscope (FE-SEM) image of the SECCM scan area is shown in Figure 3a where residues from the SECCM hops can be seen on the surface,

and assist in precisely identifying the SECCM scan area. The topography of the scanned area, obtained by SECCM (Figure 3b) correlates well with the FE-SEM image (Figure 3a), and indicate that the film aggregate is ~ 1 µm in height.

In order to produce spatially resolved SECCM images of the surface photo-electrochemical activity (i_{Surf}) under dark conditions and under illumination, the last 100 ms (see SI, section S1) of each segment of the localized transient (LED on and off) was averaged for each hop. Four complementary images can be produced from data that are recorded simultaneously: two maps from the dc components of i_{Surf} under dark conditions (Figure 3c) and under illumination (Figure 3d), and another two from the ac components of i_{Surf} (ac) (due to the ac modulation of the LED intensity), detected with the lock-in amplifier, in the dark (Figure 3e) and under illumination (Figure 3f).

The images under dark conditions (Figures 3c and 3e) highlight the low noise level of the setup (note the difference in dark and illuminated current scales). A strong spatial correlation appears between the SEM image in Figure 3a and the (photo)activity maps in Figure 3d and 3f. As we aimed to increase the signal-to-noise for the i_{Surf} (ac) amplitude measurements, a time constant of 1 second for the lock-in amplifier was chosen (sufficiently longer than the intensity modulation frequency). In future work, on other systems, optimization of the frequency of light modulation and time constant settings may allow a full analysis of the ac amplitude and phase components so that IMPS techniques could be implemented. It is important to point out that photocurrents produced from films with a thickness of less than a micron, are detectable in the setup herein, providing a significant improvement compared to the sensitivity of previous local measurements.[31-33] The external quantum efficiency (EQE) can be calculated for each hop, providing valuable localized information. The EQE calculated for the highest photo-electrochemical current recorded (~ 200 fA) in the scanned area corresponds to 0.8 % (SI, section S4 for calculation), suggesting

that even thin sensitized films (< 2 μm) can yield relatively high conversion efficiencies, in agreement with previous macroscopic studies.[34]

In situ growth and photoelectrochemical characterization of P3HT films on transparent Au substrates

To demonstrate the capability of in-situ photo-electrochemical characterization of minimal organic material, we grew P3HT electrochemically[35,36] on a transparent Au substrate,[37] using cyclic voltammetry in a SECCM setup (see SI, section S5 for CVs). In order to provide in-situ measurements of the freshly deposited P3HT film, the photocurrents were measured with the same tip used for deposition (i.e. a tip containing the 3HT monomer). Since the polymerization of P3HT is known to suffer from the presence of water,[38] the experiments were performed using an environmental cell with N_2 gas flowed in to assist in the drying of the meniscus. For photocurrent characterization, a bottom illumination configuration was adopted and the LED intensity was set to a fixed value (without intensity modulation).

The (photo)electrochemical response and corresponding FE-SEM image of the deposited film are shown in Figure 4. During the photocurrent measurement the surface was held at 0 V vs Ag QRCE (a potential range where the polymer is known to be un-doped).[36] A cathodic photocurrent transient was observed due to minority carrier generation (electrons) upon illumination ($3 \leq t \leq 7$ s), which led to the reduction of dissolved oxygen in the tip solution. Importantly the noise level during the photocurrent measurement is only ~ 6 fA, which permits the (photo)electrochemical response (~ 30 fA) to be clearly resolved during illumination. The FE-SEM image reveals a small amount of film on the Au substrate, roughly the size of the SECCM tip footprint (4.6 μm and 2.2 μm major and minor axis, respectively). The capability of measuring such low (photo)responses from minimal amounts of material

further highlights the use of photo-SECCM for studying thin molecular or organic materials at the micro to nanoscale.

Conclusions

An SECCM platform has been described that enables the investigation of (photo)electrochemical systems at the micro to nanoscale with high sensitivity. The high spatial resolution achieved with SECCM (photo)electrochemical imaging has been coupled with ultrasensitive measurements at the tens of fA range, opening up prospects for accessing a wide range of (photo)electrochemical phenomena, with future applications, such as assessing materials for solar energy conversion, water treatment, bio-sensing and photosynthesis.

A variety of substrates can be investigated with top and bottom illumination and the LED could be easily replaced to access different spectral regions (for example, UV illumination for semiconductors with a wide band gap) as well as infra-red. SECCM coupled with photo-illumination should be useful as a rapid in-situ screening technique. All of these features offer significant opportunity in nanoscale (photo)electrochemistry, and can be employed together with complementary microscopy techniques in a multi-microscopy approach on the same region of a sample. Furthermore, ac photocurrent techniques such as IMPS methods could be implemented at the nanoscale, in the future.

Associated content

SECCM photo-illumination setup, Sample preparation and solutions, SECCM control experiments for dye sensitized TiO_2 films, External quantum efficiency (EQE),

Electrochemical deposition of P3HT on transparent Au substrates. This material is available free of charge via the Internet at http://pubs.acs.org

Author information

Corresponding Author

* p.r.unwin@warwick.ac.uk

Notes

The authors declare no competing financial interest.

Table of Contents (TOC)

References

(1)   Rodríguez, J. A.; Fernández-Garcia, M. *Synthesis, Properties, and Applications of Oxide Nanomaterials*; John Wiley & Sons: New Jersey, 2007.

(2)   Lai, S. C. S.; Macpherson, J. V.; Unwin, P. R. *MRS Bulletin* **2012**, *37*, 668.

(3)   Wang, Z.-S.; Sayama, K.; Sugihara, H. *J. Phys. Chem. B* **2005**, *109*, 22449.

(4)   Lee, J.; Ye, H.; Pan, S.; Bard, A. J. *Anal. Chem.* **2008**, *80*, 7445.

(5)   Amemiya, S.; Bard, A. J.; Fan, F.-R. F.; Mirkin, M. V.; Unwin, P. R. *Annu. Rev. Anal. Chem.* **2008**, *1*, 95.

(6)   Wittstock, G.; Burchardt, M.; Pust, S. E.; Shen, Y.; Zhao, C. *Angew. Chem. Int. Ed.* **2007**, *46*, 1584.

(7)   Zhang, F.; Roznyatovskiy, V.; Fan, F.-R. F.; Lynch, V.; Sessler, J. L.; Bard, A. J. *J. Phys. Chem. C* **2011**, *115*, 2592.

(8)   Yuan, D.; Xiao, L.; Jia, J.; Zhang, J.; Han, L.; Li, P.; Mao, B.-W.; Zhan, D. *Anal. Chem.* **2014**.

(9)   Fernando, A.; Parajuli, S.; Alpuche-Aviles, M. A. *J. Am. Chem. Soc.* **2013**, *135*, 10894.

(10)   Haram, S. K.; Bard, A. J. *J. Phys. Chem. B* **2001**, *105*, 8192.

(11)   Park, H. S.; Leonard, K. C.; Bard, A. J. *J. Phys. Chem. C* **2013**, *117*, 12093.

(12)   Kylberg, W.; Wain, A. J.; Castro, F. A. *J. Phys. Chem. C* **2012**, *116*, 17384.

(13)   Martin, C. J.; Bozic-Weber, B.; Constable, E. C.; Glatzel, T.; Housecroft, C. E.; Wright, I. A. *Electrochim. Acta* **2014**, *119*, 86.

(14)   Güell, A. G.; Meadows, K. E.; Dudin, P. V.; Ebejer, N.; Macpherson, J. V.; Unwin, P. R. *Nano Lett.* **2013**.

(15)   Güell, A. G.; Ebejer, N.; Snowden, M. E.; McKelvey, K.; Macpherson, J. V.; Unwin, P. R. *Proc. Natl. Acad. Sci. U. S. A.* **2012**, *109*, 11487.

(16)   Kleijn, S. E. F.; Lai, S. C. S.; Miller, T. S.; Yanson, A. I.; Koper, M. T. M.; Unwin, P. R. *J. Am. Chem. Soc.* **2012**, *134*, 18558.

(17)   Kollender, J. P.; Gasiorowski, J.; Sariciftci, N. S.; Mardare, A. I.; Hassel, A. W. *J. Phys. Chem. C* **2014**, *118*, 16919.

(18)   Ebejer, N.; Güell, A. G.; Lai, S. C. S.; McKelvey, K.; Snowden, M. E.; Unwin, P. R. *Annu. Rev. Anal. Chem.* **2013**, *6*, 329.

(19)   Ebejer, N.; Schnippering, M.; Colburn, A. W.; Edwards, M. A.; Unwin, P. R. *Anal. Chem.* **2010**, *82*, 9141.

(20)   Snowden, M. E.; Güell, A. G.; Lai, S. C. S.; McKelvey, K.; Ebejer, N.; O'Connell, M. A.; Colburn, A. W.; Unwin, P. R. *Anal. Chem.* **2012**, *84*, 2483.

(21)   Aaronson, B. D. B.; Chen, C.-H.; Li, H.; Koper, M. T. M.; Lai, S. C. S.; Unwin, P. R. *J. Am. Chem. Soc.* **2013**, *135*, 3873.

(22)   Aaronson, B. D. B.; Lai, S. C. S.; Unwin, P. R. *Langmuir* **2014**, *30*, 1915.

(23)   Güell, A. G.; Ebejer, N.; Snowden, M. E.; Macpherson, J. V.; Unwin, P. R. *J. Am. Chem. Soc.* **2012**, *134*, 7258.

(24)   Kirkman, P. M.; Güell, A. G.; Cuharuc, A. S.; Unwin, P. R. *J. Am. Chem. Soc.* **2013**, *136*, 36.

(25)   McKelvey, K.; O'Connell, M. A.; Unwin, P. R. *Chem. Commun.* **2013**, 2986.

(26)   Williams, C. G.; Edwards, M. A.; Colley, A. L.; Macpherson, J. V.; Unwin, P. R. *Anal. Chem.* **2009**, *81*, 2486.

(27)   Peter, L. M. *J. Phys. Chem. C* **2007**, *111*, 6601.

(28)   Laslau, C.; Williams, D. E.; Kannan, B.; Travas-Sejdic, J. *Adv. Funct. Mater.* **2011**, *21*, 4607.

(29)   Dloczik, L. *J. Phys. Chem. B* **1997**, *101*, 10281.

(30)   Walker, A. B.; Peter, L. M.; Lobato, K. *Chimia* **2007**, *61*, 792.

(31)   Jiu, J.; Isoda, S.; Wang, F.; Adachi, M. *J. Phys. Chem. B* **2006**, *110*, 2087.

(32)   Kang, M. G.; Ryu, K. S.; Chang, S. H.; Nam Gyu Park; Hong, J. S.; Kim, K.-J. *Bull. Korean Chem. Soc.* **2004**, *25*, 742.

(33)   Kao, M. C.; Chen, H. Z.; Young, S. L.; Kung, C. Y.; Lin, C. C. *Thin Solid Films* **2009**, *517*, 5096.

(34)   Ahn, S. H.; Park, J. T.; Koh, J. K.; Roh, D. K.; Kim, J. H. *Chem. Commun.* **2011**, *47*, 5882.

(35)   Hillman, A. R.; Mallen, E. F. *J. Electroanal. Chem.* **1987**, *220*, 351.

(36)   Ratcliff, E. L.; Jenkins, J. L.; Nebesny, K.; Armstrong, N. R. *Chem. Mater.* **2008**, *20*, 5796.

(37)   Stec, H. M.; Hatton, R. A. *Advanced Energy Materials* **2013**, *3*, 193.

(38)   Heinze, J.; Frontana-Uribe, B. A.; Ludwigs, S. *Chem. Rev.* **2010**, *110*, 4724.
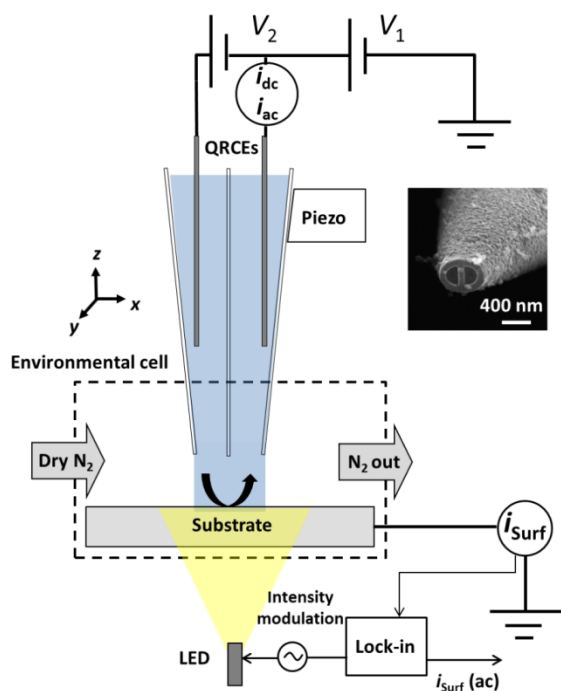
Figure 1 Schematic of SECCM with illumination. A dual barrel glass pipet pulled to a fine point serves as a local probe. A field emission scanning electron microscope (FE-SEM) image of a typical probe (450 nm diameter, corresponding to an aerial footprint of 1.6×10^{-9} cm^2) is shown in the inset. The working electrode potential ($V_{Surf} = - V_1 - V_2/2$)) was varied by changing V_1 and the resulting surface current (i_{Surf}) was recorded. An LED was used in either a bottom (as shown) or top illumination configuration. A bias potential (V_2) of +0.15 V was applied between two Ag quasi-reference counter electrodes (QRCEs) resulting in a conductance current (i_{dc}). A second external lock-in amplifier was used for light intensity modulation and was measured at the same frequency (i_{Surf} (ac)).
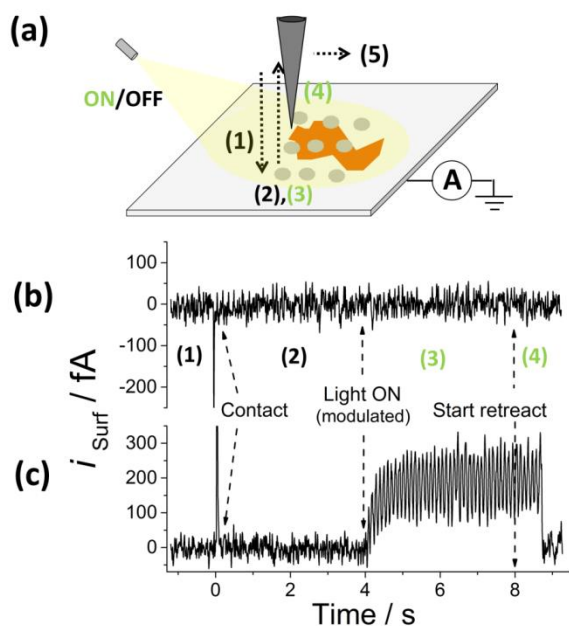
Figure 2 Schematic of photo-SECCM hopping scan (a): approach to surface with light OFF (1), hold time, of 4 seconds, on the surface with the LED OFF (2), hold time, of 4 seconds, on the surface with the LED ON (3), retract from surface (4), and move to new hop (5). Typical SECCM transients (surface current (i_{Surf}) vs time) of hop measurements with a tip containing 13 mM tetrabutylammonium iodide in 1-butyl-3-methylimidazolium tetrafluoroborate [BMIm][BF$_4$] on: non- photo-active HOPG substrate (b) and photoactive drop casted N719 sensitized TiO$_2$ films (c). The surface was held at a potential of + 0.4 V vs Ag QRCE and the light intensity was modulated at 9 Hz using a lock-in amplifier.
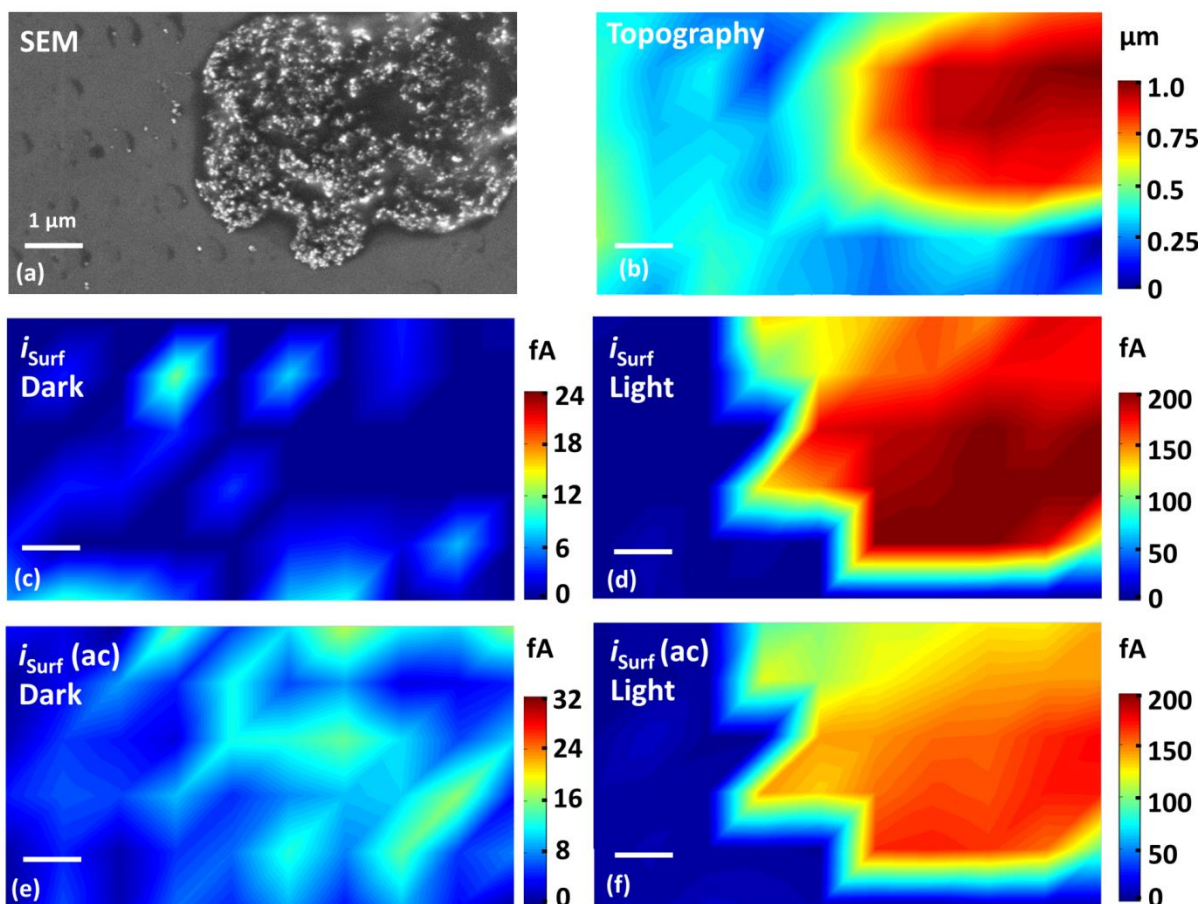
Figure 3 SECCM hopping mode scan of N719 sensitized TiO_2 film on HOPG: FE-SEM image of the scanned area (a), SECCM topography map (b). Surface DC SECCM maps: in the dark (~ 20 fA noise level) (c), and under ac illumination (d), ac component of surface current in the dark (i_{Surf} (ac)) (e), and under ac magnitude modulated illumination (f). The tip contained 13 mM tetrabutylammonium iodide in 1-butyl-3-methylimidazolium tetrafluoroborate. The surface was held at + 0.4 V vs Ag and the light intensity modulated at 9 Hz from 0 to 33 mW cm^{-2}. All scale bars are 1 μm.
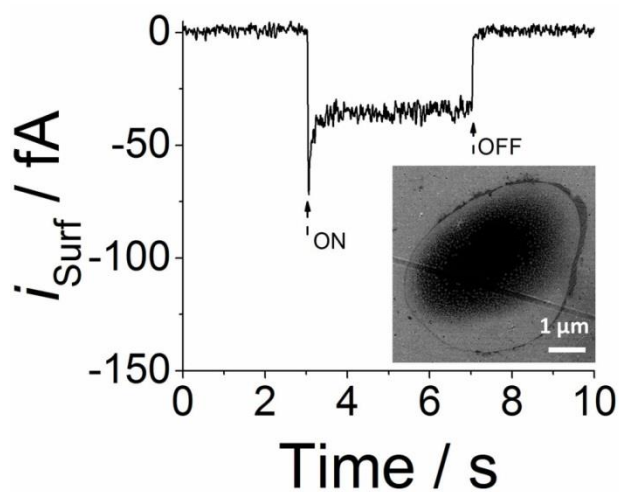
Figure 4 SECCM surface (photo)current-time transients on a P3HT film deposited on a transparent Au substrate. The surface was held at 0.0 V vs Ag QRCE during the measurements. The light source was switched ON at t = 3 seconds and then OFF at t = 7 seconds. The SECCM tip (4.6 μm and 2.2 μm major and minor axis, respectively) contained 0.1 M 3-hexyl thiophene in a 1:1 (v/v) mixture of [BMIm][BF$_4$] and dried acetonitrile. A FE-SEM image of the P3HT film is shown in the inset.